

A role for mitochondria in NLRP3 inflammasome activation

Rongbin Zhou¹, Amir S. Yazdi¹, Philippe Menu¹ & Jürg Tschopp¹

An inflammatory response initiated by the NLRP3 inflammasome is triggered by a variety of situations of host ‘danger’, including infection and metabolic dysregulation^{1,2}. Previous studies suggested that NLRP3 inflammasome activity is negatively regulated by autophagy and positively regulated by reactive oxygen species (ROS) derived from an uncharacterized organelle. Here we show that mitophagy/autophagy blockade leads to the accumulation of damaged, ROS-generating mitochondria, and this in turn activates the NLRP3 inflammasome. Resting NLRP3 localizes to endoplasmic reticulum structures, whereas on inflammasome activation both NLRP3 and its adaptor ASC redistribute to the perinuclear space where they co-localize with endoplasmic reticulum and mitochondria organelle clusters. Notably, both ROS generation and inflammasome activation are suppressed when mitochondrial activity is dysregulated by inhibition of the voltage-dependent anion channel. This indicates that NLRP3 inflammasome senses mitochondrial dysfunction and may explain the frequent association of mitochondrial damage with inflammatory diseases.

The NLRP3 inflammasome is a molecular platform activated upon signs of cellular ‘danger’ to trigger innate immune defences through the maturation of pro-inflammatory cytokines such as interleukin (IL)-1 β ¹. Strong associations of a number of human heritable and acquired diseases with dysregulated inflammasome activity highlight the importance of the NLRP3 inflammasome in regulating immune responses³. Key components of a functional NLRP3 inflammasome are NLRP3, the adaptor protein ASC and caspase-1 (ref. 1). Upon detecting cellular stress, NLRP3 recruits ASC and procaspase-1, which results in caspase-1 activation and processing of cytoplasmic targets, including the pro-inflammatory cytokines IL-1 β and IL-18.

A wide variety of danger signals activate the NLRP3 inflammasome. These include pathogen-associated molecular patterns⁴ and host-derived molecules that are indicative of cellular damage (danger-associated molecular patterns) such as uric-acid crystals¹. The mechanisms by which these structurally distinct molecules trigger NLRP3 inflammasome activation are currently unclear. One of the models proposes that NLRP3 is activated by a common pathway of ROS⁵. The source of ROS is currently unclear, but we previously suggested the involvement of one or several of the seven known NADPH oxidases⁵. However, macrophages deficient in subunits specific to three of the seven NADPH oxidases, that is, NOX1, NOX2 and NOX4, respond normally to inflammasome activators (C. Dostert and J.T., unpublished observations) or have even slightly increased activity⁶, which suggests a possible role of other NADPH oxidase members or functional redundancy. Alternatively, further ROS required for inflammasome activation could be generated by other cellular sources.

The main source of cellular ROS is mitochondria. Various stress conditions, including increased metabolic rates, hypoxia, or membrane damage all markedly induce mitochondrial ROS production⁷. To investigate a possible implication of mitochondria in inflammasome activation, we artificially induced ROS production in mitochondria by blocking key enzymes of the respiratory chain. Complex I is one of the main sites at which electrons can leak to oxygen and result in superoxide

production⁷. In agreement with previous reports⁸, addition of the complex I inhibitor rotenone resulted in the loss of mitochondrial membrane potential and robust ROS production (Fig. 1a, b). This was determined using three types of mitochondria-specific labels that distinguish respiring (Mitotracker deep red), total (Mitotracker green) and ROS-generating mitochondria (MitoSOX) (Fig. 1a, b). ROS-generating mitochondria were also observed when complex III was inhibited by antimycin A, whereas the complex II inhibitor thenoyltrifluoroacetone (TTFA) had only a minor effect (Fig. 1a, b).

A correlation between mitochondrial ROS activity and the presence of active IL-1 β in the supernatant of the human THP1 macrophage cell line was observed. Whereas rotenone- or antimycin-treated cells showed increased IL-1 β secretion in a dose-dependent manner, no or little cytokine was detectable if cells were treated with TTFA (Fig. 1c). In THP1 cells with knocked-down NLRP3 or caspase-1, or in bone-marrow-derived macrophages (BMDMs) from *Nlrp3*^{-/-} mice, the respiratory chain inhibitors did not induce IL-1 β or caspase-1 secretion (Fig. 1d and Supplementary Fig. 1a). In contrast, macrophages lacking the IPAF/NLRC4 inflammasome responded in a similar way to wild-type cells, indicating that activation of caspase-1 and processing and secretion of IL-1 β by inhibitors of the respiratory chain were mediated by the NLRP3 inflammasome but not the IPAF inflammasome. As previously observed for MSU, activation of the NLRP3 inflammasome by rotenone and antimycin was blocked by the ROS inhibitor APDC (Supplementary Fig. 1b). Although inhibition of complex I and III activity leads to robust ROS production, damage of the mitochondria and decrease of membrane potential appeared to be partial and did not result in cell death (Supplementary Fig. 2). Consistent with this, complete breakdown of the mitochondrial membrane potential induced by high doses of the respiratory chain uncoupler CCCP did cause only little ROS production and IL-1 β release. Nonetheless, CCCP used at a lower concentration that only partially impairs the membrane potential also spontaneously led to NLRP3 inflammasome activation (Supplementary Fig. 2). These data are compatible with the notion that ROS generated by mitochondria having reduced membrane potential can lead to NLRP3 inflammasome activation.

To avoid cellular damage, ROS-generating mitochondria are constantly removed by mitophagy, a specialized process of autophagy⁹. In agreement with this established mechanism of mitochondrial disposal, autophagy-associated LC3 puncta were found to accumulate around mitochondria after the addition of rotenone (Fig. 2a). We therefore speculated that inhibition of mitophagy/autophagy should lead to the accumulation of ROS-producing damaged mitochondria, and as a consequence, to the activation of the inflammasome. To this end, the mitophagy/autophagy inhibitor 3-methyladenine (3-MA) was added to THP1 macrophages, which, as expected, resulted in the accumulation of damaged mitochondria and increased concentrations of mitochondrial ROS (Fig. 2b and Supplementary Fig. 3a). Similar to mitochondrial respiratory chain inhibition, 3-MA-induced ROS generation was paralleled by the dose-dependent secretion of IL-1 β within 6 h of mitophagy/autophagy inhibition (Supplementary Fig. 3b), which was blocked by the antioxidant APDC (Supplementary Fig. 3c). Processing

¹Department of Biochemistry, Center of Immunity and Infection, University of Lausanne, Chemin des Boveresses 155, CH-1066 Epalinges, Switzerland.

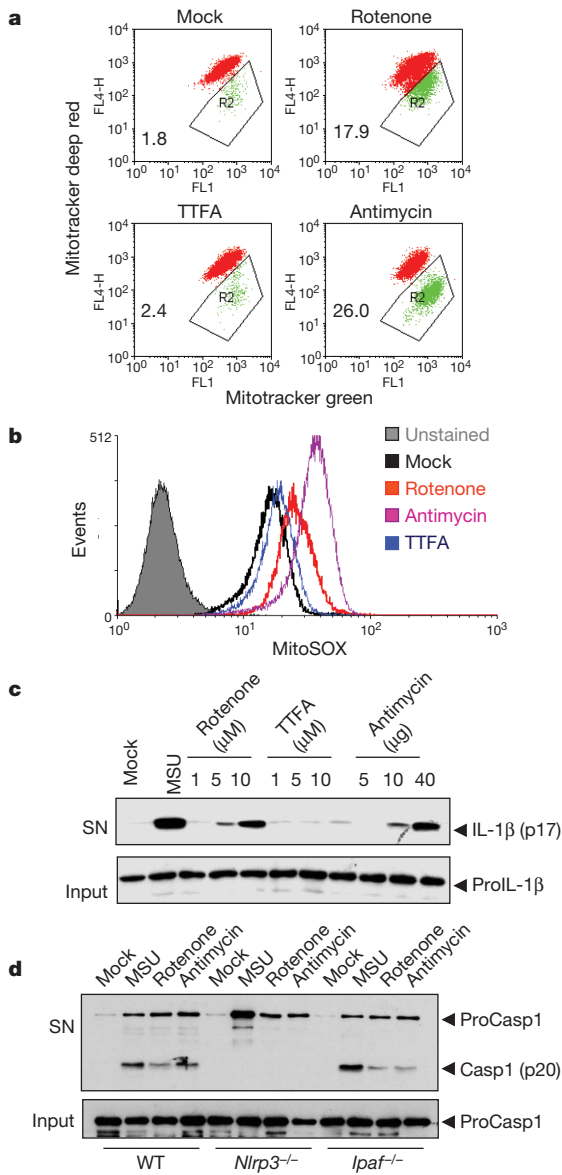


Figure 1 | Mitochondrial ROS can trigger NLRP3 inflammasome activation. **a, b**, THP1 cells were stimulated with rotenone (10 μ M), TTFA (10 μ M) or antimycin (40 μ g ml⁻¹) for 6 h and then stained with Mitotracker green and Mitotracker deep red (**a**) or MitoSOX (**b**) for 30 min and analysed by flow cytometry. **c**, THP1 cells were stimulated for 6 h with the indicated amounts of rotenone, TTFA or antimycin. Supernatants (SN) and cell extracts (input) were analysed by western blotting as indicated. **d**, LPS-primed bone-marrow-derived macrophages (BMDMs) from wild-type (WT), *Nlrp3* or *Ipaf* deficient mice were stimulated for 6 h with MSU (150 μ g ml⁻¹), rotenone (10 μ M for THP1 cells and 40 μ M for BMDMs) or antimycin (40 μ g ml⁻¹ for THP1 cells and 10 μ g ml⁻¹ for BMDMs). The release of caspase-1 (western blot) was then determined. Data shown are representative of three independent experiments.

of proIL-1 β caused by the blockade of mitophagy/autophagy was NLRP3- and ASC-dependent and not reliant on the IPAF inflammasome (Fig. 2d).

Because most pharmacological drugs have off-target effects, we next inhibited mitophagy/autophagy specifically through downregulation of two proteins that have crucial functions in mitophagy/autophagy, that is, beclin 1, a Bcl-2- and PI3KIII-interacting protein, and ATG5, a protein essential for autophagosome formation¹⁰. In contrast to the pharmacological inhibitors, spontaneous inflammasome activation was less efficient, as cells with knocked down beclin 1 and ATG5 had to be cultured for 24 h before we could detect active IL-1 β in the culture supernatant (Fig. 2d, e). Inhibition of mitophagy/autophagy through downregulation of beclin 1 or ATG5 also sensitized macrophages for the release of IL-1 β induced by MSU or nigericin (Fig. 2e). This augmented response was not associated with increased cell death (Supplementary Fig. 3d). It is therefore feasible that a functional mitophagy/autophagy system acts as a scavenger of mitochondrial ROS through removal of damaged mitochondria and thereby suppresses NLRP3 inflammasome activation.

ROS are short-lived and can act as a signalling messenger only for a short distance¹¹. Thus, NLRP3 should ideally be localized in close vicinity to mitochondria, allowing efficient sensing of the presence of damaged ROS-generating mitochondria. Of the 22 NLR members, only one, NOD5 (also called NLRX1), has a predicted mitochondrial import sequence and thus resides in the mitochondria^{12,13}. Using confocal microscopy, the localization of NLRP3 in THP1 macrophages was examined. Under non-stimulatory conditions, most NLRP3 protein was found to localize to cytoplasmic granular structures (Fig. 3). Further analysis showed a significant overlap of NLRP3 with the

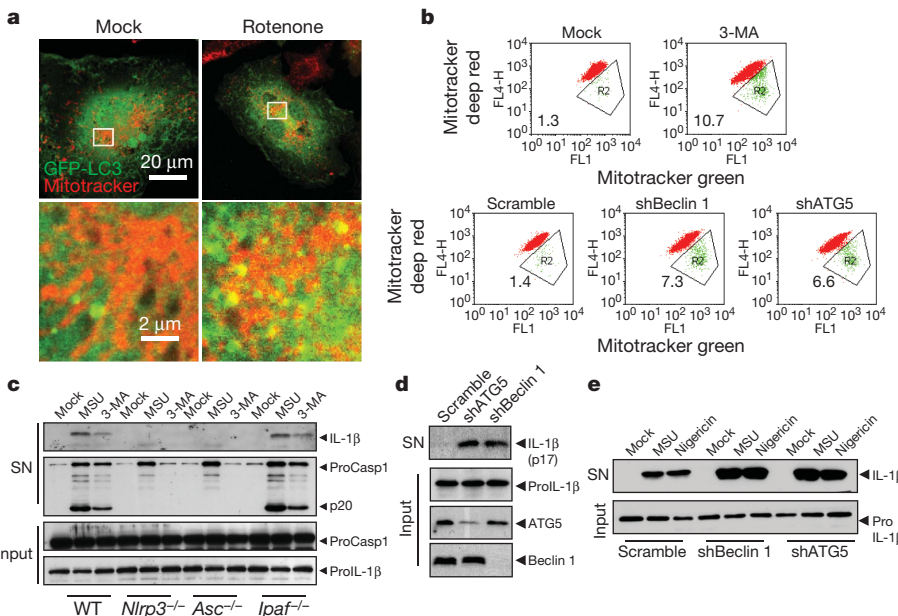


Figure 2 | Inhibition of autophagy/mitophagy results in ROS generation and inflammasome activation. **a**, BMDMs expressing GFP-LC3 were stimulated with rotenone (40 μ M) for 3 h and the co-localization of mitochondria and GFP-LC3 dots were analysed using confocal microscopy. **b**, THP1 cells stimulated with 3-methyladenine (3-MA, 10 mM) for 24 h or THP1 cells stably expressing shRNA against beclin 1 or ATG5 were stained with Mitotracker green and Mitotracker deep red for 30 min, and analysed by flow cytometry. **c**, LPS-primed BMDMs from wild-type, *Nlrp3*^{-/-}, *Asc*^{-/-} or *Ipaf*^{-/-} knockout mice were stimulated with MSU (150 μ g ml⁻¹) or 3-MA (10 mM) for 6 h and the release of active caspase-1 and IL-1 β was determined. **d**, THP1 cells stably expressing shRNA against beclin 1 or ATG5 were incubated for 24 h and media supernatants (SN) and inputs were analysed by western blotting. **e**, THP1 cells stably expressing shRNA against beclin 1 or ATG5 were stimulated with MSU or nigericin for 6 h. Data shown are representative of three independent experiments.

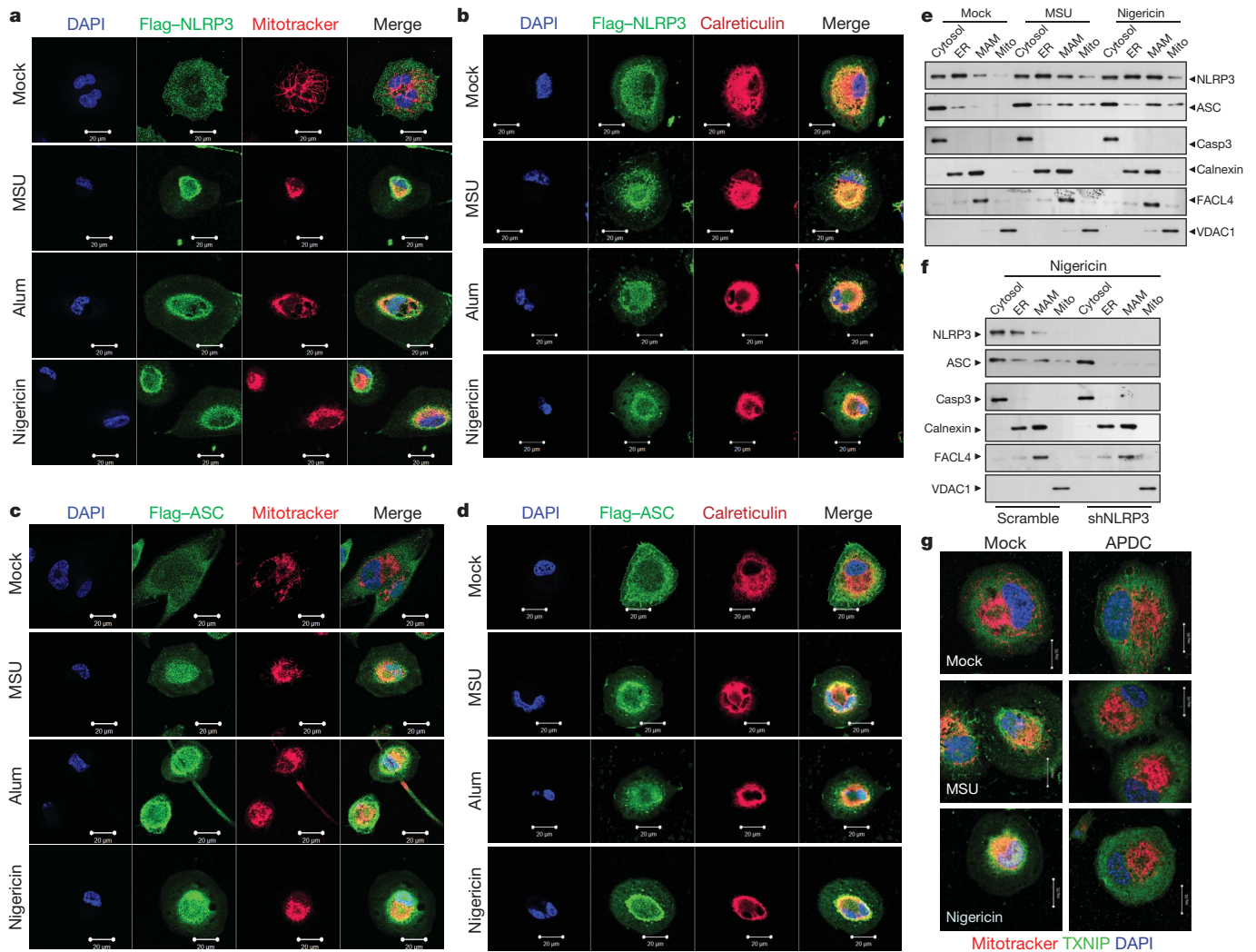


Figure 3 | Co-localization of the NLRP3 inflammasome components and endoplasmic retulum-mitochondria. **a–d**, THP1 cells expressing Flag-NLRP3 (**a, b**) or Flag-ASC (**c, d**) were analysed for the co-localization of Flag-NLRP3 with the endoplasmic reticulum (ER) marker calreticulin or mitochondria (Mitotracker) using confocal microscopy. **e**, THP1 cells were stimulated with MSU or nigericin and then fractionated. The cytosolic, ER, MAM and mitochondrial fractions were analysed by western blotting as

indicated in the text. **f**, THP1 cells stably expressing shRNA against NLRP3 were stimulated with nigericin and subcellular fractions analysed as in **e**. **g**, TXNIP associates with mitochondria after NLRP3 inflammasome activation in a ROS-dependent manner. THP1 cells were stimulated with MSU and nigericin, and TXNIP localization was investigated in the presence or absence of the antioxidant APDC. Data shown are representative of two or three independent experiments. Scale bars: **a–g**, 20 μ m.

endoplasmic reticulum (ER) marker calreticulin, whereas no or very little co-localization was detected with Mitotracker, the Golgi marker Giantin or the lysosome/phagosome staining dye lysotracker (Fig. 3a, b and Supplementary Fig. 4). Primarily ER and not mitochondrial staining of NLRP3 was also detected when cells were analysed by electron microscopy (Supplementary Fig. 5). This localization changed significantly after inflammasome stimulation with MSU, alum or nigericin. NLRP3 relocated into the perinuclear space and co-localized with structures that stained positively for both the ER and mitochondria (Fig. 3a, b and Supplementary Fig. 6). A similar perinuclear, ER/mitochondria localization was detected for ASC after NLRP3 activation, although in contrast to NLRP3 most ASC was observed in the cytoplasm in resting cells (Fig. 3c, d and Supplementary Figs 4 and 6).

To confirm the NLRP3 association with the ER/mitochondria observed by microscopy, subcellular fractionation studies were performed. With this approach, NLRP3 was detected in both ER and cytoplasmic fractions in a roughly similar amount (Fig. 3e). ER membranes can tightly associate with mitochondria forming mitochondria-associated ER membranes (MAMs). MAMs are important, among other functions, in transferring lipids and Ca^{2+} from the ER to the mitochondria¹⁴. Addition of MSU and, in particular, nigericin induced

NLRP3 to associate partly with MAMs (Fig. 3e). In contrast to NLRP3, the majority of the ASC was found in the cytoplasmic fraction before inflammasome activation, and only a very minor portion of ASC was associated with the ER fraction. On stimulation with MSU or nigericin, however, the amount of ASC found in the mitochondrial fraction and particularly in the MAMs fraction increased considerably. ASC translocation to the MAMs and mitochondria was NLRP3 dependent, as no or little translocation was found in nigericin-activated THP1 cells in which NLRP3 was downregulated by short hairpin (sh)RNA (Fig. 3f).

We have previously reported that TXNIP, a protein implicated in type 2 diabetes, associated with NLRP3 in a ROS-dependent manner after its detachment from thioredoxin¹⁵. We therefore anticipated that TXNIP translocates to MAMs/mitochondria on NLRP3 inflammasome activation. Consistent with this idea, MSU and nigericin induced TXNIP to redistribute to mitochondria in a ROS-dependent manner (Fig. 3g), in agreement with a recently published report¹⁶.

Although the above results indicated that the prolonged presence of damaged and ROS-producing mitochondria might be implicated in inflammasome activation, the evidence was still indirect. We therefore sought to obtain more direct proof by inhibiting the activity of voltage-dependent anion channels (VDAC), which are the most abundant

proteins of the outer mitochondrial membrane and the major channels for the exchange of metabolites and ions between the mitochondria and other cellular compartments including the ER¹⁷. As such, the three VDAC isoforms are important regulators of mitochondrial metabolic activity, which is ultimately required for ROS production. We down-regulated expression of each of the three human VDAC isoforms by shRNA (Supplementary Fig. 7a) and measured inflammasome activation by MSU, R837, silica, alum and nigericin (Fig. 4a). In cells with knocked-down VDAC1, caspase-1 activation and IL-1 β secretion were considerably impaired for all inflammasome activators examined. As a consequence of VDAC1 knockdown, mitochondrial ROS was highly diminished (Supplementary Fig. 8). In contrast to the NLRP3 inflammasome, VDAC1 was not essential for the activation of the IPAF or the AIM2 inflammasome (Supplementary Fig. 7b). A significant reduction of IL-1 β secretion was also seen in cells where VDAC2 was knocked down (Fig. 4b). In all cases, impairment was seen with two distinct shRNA constructs (Supplementary Fig. 7). In contrast to VDAC1 and VDAC2, downregulation of VDAC3 had no effect on NLRP3 inflammasome activity (Supplementary Fig. 7c). The absence of VDAC1 also inhibited MSU- or nigericin-induced NLRP3 translocation to perinuclear areas (Fig. 4c).

VDAC activity is regulated by hexokinase and Bcl-2 family members¹⁷. Overexpression of Bcl-2 leads to partial VDAC closure and a concomitant decrease of mitochondrial Ca²⁺ levels and ROS production. We therefore examined whether increased Bcl-2 levels would have an impact on NLRP3 inflammasome activity and found that in supernatants of MSU-, alum- or nigericin-stimulated macrophages isolated from Bcl-2-overexpressing transgenic mice, IL-1 β levels were decreased when compared to cells from wild-type mice (Supplementary Fig. 9a). In contrast, no influence of Bcl-2 was detectable on *Salmonella*-mediated IPAF-inflammasome activity (Supplementary Fig. 9a) or LPS-mediated tumour-necrosis factor (TNF) secretion (Supplementary Fig. 9b).

It is now widely recognized that, apart from bioenergetic ATP production, mitochondria also have a crucial role in cell signalling events such as apoptotic cell death. Apoptotic signal transmission to the mitochondria results in the efflux of a number of potential apoptotic regulators such as cytochrome *c* to the cytosol that trigger caspase activation and lead to cell death. Our results now provide evidence for an unanticipated additional role of mitochondria, namely the orchestration of the inflammatory response.

Mitochondria are the major source of cellular ROS and it is therefore not completely unexpected that we found mitochondrial ROS capable

of NLRP3 inflammasome activation. This notion is based on the following observations: (1) inhibition of complex I or III of the mitochondrial respiratory chain, known to result in ROS generation, causes unprompted NLRP3 inflammasome activation; (2) inhibition of mitophagy/autophagy, resulting in the prolonged presence of damaged, ROS-generating mitochondria, leads to spontaneous inflammasome activation; (3) NLRP3 and ASC co-localize with mitochondria and MAMs in the presence of NLRP3 inflammasome activators; (4) knock down by shRNA or inhibition by Bcl-2 of VDAC ion channels that are crucial in mitochondrial activity and ROS generation significantly impair NLRP3 inflammasome activation. The dependence on VDAC is specific for the NLRP3 inflammasome and is not seen with the AIM2 or IPAF inflammasomes, indicating that the signalling pathways leading to their activation are distinct.

VDAC is essential for the uptake of Ca²⁺ into the mitochondria from MAMs to promote mitochondrial metabolic activity¹⁷. Upon NLRP3 inflammasome activation, a substantial portion of the inflammasome is associated to MAMs, indicating that NLRP3 checks and modulates mitochondrial activity.

There is a large amount of literature proposing a link between mitochondrial malfunction, ROS and chronic inflammatory diseases. Damage to mitochondria is now understood to have a role in the pathogenesis of a wide range of seemingly unrelated disorders¹⁸. For example, mutations in PINK1, PARKIN and DJ-1 are frequent causes of recessive Parkinson's disease. Both PINK1 and PARKIN are crucial in the removal of damaged mitochondria by mitophagy, whereas DJ-1 is localized to mitochondria and has a role in oxidative stress protection. Mutations in proteins involved in mitophagy/autophagy, such as ATG16 and IRGM, are also frequently found in Crohn's disease¹⁹. In line with this, increased IL-1 β production is observed in mice deficient in the autophagy gene *ATG16* (ref. 20). It is, however, unlikely that inhibition of mitophagy is generally used as a means to activate the NLRP3 inflammasome signalling pathway. In our opinion, a more direct mechanism, that is, an excessive induction of mitochondrial oxidative phosphorylation, is more likely.

Taken together, our data unravel unexpected mechanistic parallels between signalling pathways leading to apoptosis and inflammation. In both instances, signals converge at the level of mitochondria where VDAC activity seems to have a role for the activation of two seemingly unrelated downstream processes. VDAC is not only crucial for inflammasome activation, as shown here, but also has a role in apoptosis induction by Bax²¹. The mechanism that determines whether mitochondria

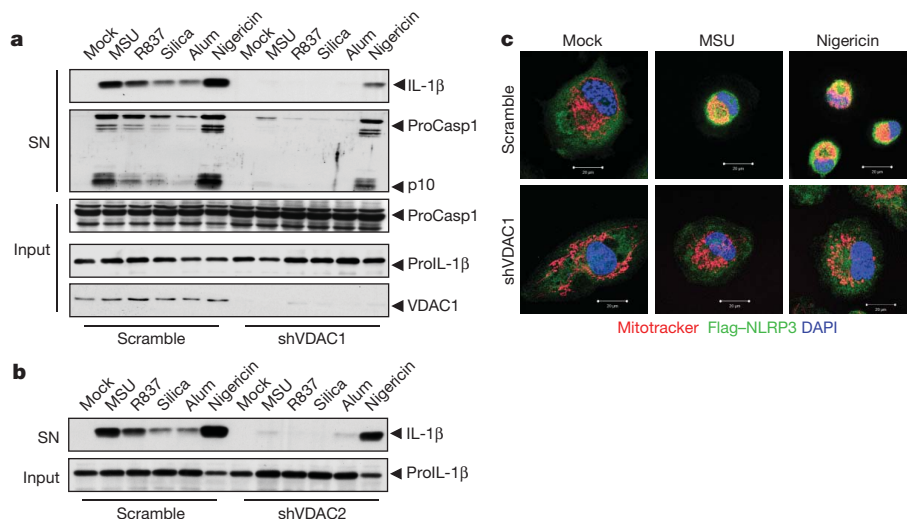


Figure 4 | VDAC is essential for NLRP3 inflammasome activation. **a**, THP1 cells stably expressing shVDAC1 were stimulated with various NLRP3 inflammasome activators and then analysed for caspase-1 activation and IL-1 β secretion. **b**, THP1 cells expressing shRNA against VDAC2 were stimulated

with MSU, R837, silica, alum or nigericin and analysed for IL-1 β secretion. **c**, THP1 cells expressing shRNA against VDAC1 were stimulated with MSU and nigericin, and NLRP3 localization was analysed by confocal microscopy. Scale bars: 20 μ m.

induce inflammasome or apoptosome assembly is currently unclear. Whereas ROS is essential for the activation of both the inflammasome and apoptosome²², apoptosome formation requires in addition cytochrome *c* release from mitochondria into the cytosol. There is no evidence for cytochrome *c* being implicated in inflammasome activation, yet it cannot be ruled out that recognition of a different protein released from partially damaged mitochondria is required. The decision to induce inflammation or apoptosis must be tightly controlled to avoid pathological conditions associated with a chronic inflammatory response. Regrettably, this control mechanism seems to be easily deranged, as shown by the many diseases that are associated with mutations in genes that affect mitochondrial function.

METHODS SUMMARY

Mice. *Nlrp3*^{-/-}, *Asc*^{-/-}, *Ipa1*^{-/-} and H2K-Bcl-2 transgenic mice were described previously^{23–25}. All mice were on a C57BL/6 background except for experiments used for NLRP1b inflammasome activation (BALB/c).

Cell fractionation. MAMs, mitochondria and microsomes were isolated from PMA-differentiated THP1 cells as previously described²⁶.

Full Methods and any associated references are available in the online version of the paper at www.nature.com/nature.

Received 25 June; accepted 11 November 2010.

Published online 1 December 2010.

- Schroder, K. & Tschopp, J. The inflammasomes. *Cell* **140**, 821–832 (2010).
- Latz, E. The inflammasomes: mechanisms of activation and function. *Curr. Opin. Immunol.* **22**, 28–33 (2010).
- Kastner, D. L., Aksentijevich, I. & Goldbach-Mansky, R. Autoinflammatory disease reloaded: a clinical perspective. *Cell* **140**, 784–790 (2010).
- Franchi, L., Munoz-Planillo, R., Reimer, T., Eigenbrod, T. & Nunez, G. Inflammasomes as microbial sensors. *Eur. J. Immunol.* **40**, 611–615 (2010).
- Dostert, C. *et al.* Innate immune activation through Nalp3 inflammasome sensing of asbestos and silica. *Science* **320**, 674–677 (2008).
- Latz, E. NOX-free inflammasome activation. *Blood* **116**, 1393–1394 (2010).
- Brookes, P. S., Yoon, Y., Robotham, J. L., Anders, M. W. & Sheu, S.-S. Calcium, ATP, and ROS: a mitochondrial love-hate triangle. *Am. J. Physiol. Cell Physiol.* **287**, C817–C833 (2004).
- Li, N. *et al.* Mitochondrial complex I inhibitor rotenone induces apoptosis through enhancing mitochondrial reactive oxygen species production. *J. Biol. Chem.* **278**, 8516–8525 (2003).
- Goldman, S. J., Taylor, R., Zhang, Y. & Jin, S. Autophagy and the degradation of mitochondria. *Mitochondrion* **10**, 309–315 (2010).
- Levine, B. & Kroemer, G. Autophagy in the pathogenesis of disease. *Cell* **132**, 27–42 (2008).
- Veal, E. A., Day, A. M. & Morgan, B. A. Hydrogen peroxide sensing and signaling. *Mol. Cell* **26**, 1–14 (2007).
- Moore, C. B. *et al.* NLRX1 is a regulator of mitochondrial antiviral immunity. *Nature* **451**, 573–577 (2008).
- Tattoli, I. *et al.* NLRX1 is a mitochondrial NOD-like receptor that amplifies NF- κ B and JNK pathways by inducing reactive oxygen species production. *EMBO Rep.* **9**, 293–300 (2008).
- Hayashi, T., Rizzuto, R., Hajnoczky, G. & Su, T. P. MAM: more than just a housekeeper. *Trends Cell Biol.* **19**, 81–88 (2009).
- Zhou, R., Tardivel, A., Thorens, B., Choi, I. & Tschopp, J. Thioredoxin-interacting protein links oxidative stress to inflammasome activation. *Nature Immunol.* **11**, 136–140 (2010).
- Saxena, G., Chen, J. & Shalev, A. Intracellular shuttling and mitochondrial function of thioredoxin-interacting protein. *J. Biol. Chem.* **285**, 3997–4005 (2010).
- Colombini, M. VDAC: the channel at the interface between mitochondria and the cytosol. *Mol. Cell. Biochem.* **256**, 107–115 (2004).
- Oliveira, J. M. Nature and cause of mitochondrial dysfunction in Huntington's disease: focusing on Huntingtin and the striatum. *J. Neurochem.* **114**, 1–12 (2010).
- Restivo, N. L., Srivastava, M. D., Schafer, I. A. & Hoppel, C. L. Mitochondrial dysfunction in a patient with crohn disease: possible role in pathogenesis. *J. Pediatr. Gastroenterol. Nutr.* **38**, 534–538 (2004).
- Saitoh, T. *et al.* Loss of the autophagy protein Atg16L1 enhances endotoxin-induced IL-1 β production. *Nature* **456**, 264–268 (2008).
- Yamagata, H. *et al.* Requirement of voltage-dependent anion channel 2 for pro-apoptotic activity of Bax. *Oncogene* **28**, 3563–3572 (2009).
- Sato, T. *et al.* Fas-mediated apoptosome formation is dependent on reactive oxygen species derived from mitochondrial permeability transition in Jurkat cells. *J. Immunol.* **173**, 285–296 (2004).
- Mariathasan, S. *et al.* Differential activation of the inflammasome by caspase-1 adaptors ASC and Ipaf. *Nature* **430**, 213–218 (2004).
- Martinon, F., Petrilli, V., Mayor, A., Tardivel, A. & Tschopp, J. Gout-associated uric acid crystals activate the NALP3 inflammasome. *Nature* **440**, 237–241 (2006).
- Domen, J., Cheshier, S. H. & Weissman, I. L. The role of apoptosis in the regulation of hematopoietic stem cells: Overexpression of Bcl-2 increases both their number and repopulation potential. *J. Exp. Med.* **191**, 253–264 (2000).
- Wieckowski, M. R., Giorgi, C., Lebiedzinska, M., Duszynski, J. & Pinton, P. Isolation of mitochondria-associated membranes and mitochondria from animal tissues and cells. *Nature Protocols* **4**, 1582–1590 (2009).

Supplementary Information is linked to the online version of the paper at www.nature.com/nature.

Acknowledgements This study was supported by grants of the Swiss National Science Foundation and by the Institute for Arthritis Research. A.S.Y. is a recipient of a stipend of the DFG. We would like to thank K. Schroder, C. Thomas and J. Vince for critical reading of the manuscript and G. W. Knott, EPFL, Lausanne, for help in collecting electron micrographs.

Author Contributions R.Z., A.S.Y. and P.M. devised and performed the experiments. J.T. supervised the work.

Author Information Reprints and permissions information is available at www.nature.com/reprints. The authors declare no competing financial interests. Readers are welcome to comment on the online version of this article at www.nature.com/nature. Correspondence and requests for materials should be addressed to J.T. (jurg.tschopp@unil.ch).

METHODS

Mice. *Nlrp3*^{-/-}, *Asc*^{-/-}, *Ipaf*^{-/-} and H2K-Bcl-2 transgenic mice were described previously^{23–25}. All mice were on a C57BL/6 background except for experiments used for NLRP1b inflammasome activation (BALB/c).

Cell fractionation. MAMs, mitochondria and microsomes were isolated from PMA-differentiated THP1 cells as previously described²⁶.

Reagents. Nigericin, rotenone, antimycin, thenoyltrifluoroacetone (TTFA), uric acid, (2R,4R)-4-aminopyrrolidine-2, 4-dicarboxylate (APDC), 3-methyladenine (3-MA), ATP, menadione, carbonyl cyanide 3-chlorophenylhydrazone (CCCP), poly(AT) and silica were purchased from Sigma. MitoSOX, Mitotracker green, Mitotracker deep red, JC-1 and lysotracker red were from Invitrogen. LDH release kits were from Roche. Ultrapure LPS and R837 were obtained from InvivoGen. Inject alum was from Pierce. *Salmonella typhimurium* is a gift from R. Van Bruggen. Anti-human proIL-1 β was produced in house. The anti-NLRP3 antibodies (Cryo-2) were from Adipogen. Anti-human cleaved IL-1 β (D116), anti-ATG5 (2630S), anti-beclin 1 (3738), anti-calnexin (2433S), anti-caspase-3 (9662) and anti-VDAC1 (4866) antibodies were purchased from Cell Signaling. Anti-ASC antibody (AL177) was from Adipogen. Anti-TXNIP (40-3700) antibody was from Invitrogen. Anti-VDAC3 antibody (sc-79341), anti-FACL-4 (sc-47997) and anti-human caspase-1 (sc-622) were from Santa Cruz. Anti-VDAC2 antibody (ab77160), anti-Giantin (ab24586), anti-GAPDH (ab8245) and anti-calreticulin (ab14234) were from Abcam. Anti-mouse IL-1 β antibody was a gift from R. Solari. Anti-mouse caspase-1 (p20) antibody was a gift from P. Vandenabeele. Anti-Flag (M2) antibody was from Sigma. *Bacillus anthracis* lethal toxin (protective antigen and lethal factor) was from List Biological Laboratories. All tissue culture reagents were from Invitrogen.

Generation of stable THP1 cells expressing Flag-NLRP3 or Flag-ASC. Retroviral vector (LZRS-MS-IRES-ZEO/PBR-Flag-NLRP3 or Flag-ASC) was co-transfected with the helper plasmids VSV-G and Hit60 into 293T cells by calcium phosphate transfection. Culture supernatants containing recombinant viral particles were harvested and used to infect THP1 cells in the presence of polybrene (8 mg ml⁻¹). To establish stable cell lines, THP1 cells were selected with zeocin (1 mg ml⁻¹) on day 3 after infection.

Transduction of GFP-LC3 in BMDMs. Lentiviral vector (plex-GFP-LC3) was co-transfected with the helper plasmids pCMV Δ R8.91 and pMDG into 293T cells by calcium phosphate transfection. Culture supernatants containing recombinant viral particles were harvested and used to infect BMDMs on day 3 after differentiation. On day 7, the cells can be used for advanced experiments.

Cell preparation and stimulation. Human THP1 cells were cultured in RPMI 1640 media, supplemented with 10% FBS. THP1 cells were differentiated for 3 h with 100 nM phorbol-12-myristate-13-acetate (PMA). Bone marrow macrophages were derived from tibia and femoral bone marrow progenitors as described²⁷, and were primed for 4 h with 100 ng ml⁻¹ Ultra-pure LPS. For the induction of inflammasome activation, 10⁶ LPS-primed bone marrow macrophages or PMA-differentiated THP1 cells plated in 12-well plates were treated with MSU (150 μ g ml⁻¹), alum (200 μ g ml⁻¹), silica (200 μ g ml⁻¹), R837 (15 μ g ml⁻¹) for 6 h or with ATP (5 mM) or nigericin (15 μ M) for 30 min. For poly(dA:dT) transfection,

poly(dA:dT) was transfected using Lipofectamine (4 μ l ml⁻¹) as per the manufacturer's protocol (Invitrogen). Cell extracts and precipitated supernatants were analysed by immunoblot.

Generation of stable THP1 cells expressing shRNA. THP1 cells stably expressing shRNA were obtained as previously described²⁸; shRNA against NLRP3 and caspase-1 plasmids has been described¹⁵ and shRNA plasmids against beclin-1, ATG5, VDAC1, VDAC2 and VDAC3 were from Sigma.

Confocal microscopy. PMA-differentiated THP1 cells were plated on coverslips for 3 days and then used for stimulation or staining with Mitotracker red (50 nM) or Lysotracker (200 nM). After washing two times with PBST, the cells were fixed with PFA 4% in PBS for 15 min and then washed three times with PBST. After permeabilization with Triton X-100 and blocking with 10% goat serum in PBS, cells were incubated with primary antibodies (in 10% goat serum) overnight at 4 °C. After washing with PBST, cells were incubated with secondary antibodies (Invitrogen) in 10% goat serum-PBS for 60 min and rinsed in PBST. Confocal microscopy analyses were carried out using a Zeiss LSM510.

Flow cytometric analyses. Mitochondrial mass was measured by fluorescence levels upon staining with Mitotracker green and Mitotracker deep red at 50 nM for 30 min at 37 °C. Mitochondria-associated ROS levels were measured by staining cells with MitoSOX at 2.5 μ M for 30 min at 37 °C. Mitochondria membrane potential was measured using the kit from Invitrogen and performed according to the manufacturer's instructions. Cells were then washed with PBS solution and resuspended in cold PBS solution containing 1% FBS for FACS analysis.

Salmonella infection. *Salmonella typhimurium* was pre-cultured on day 1. On day 2, differentiated THP1 cells were infected for 1 h with the *S. typhimurium* culture (1:100). Cells were washed and then incubated for 3 h in OptiMEM medium with gentamycin (Invitrogen).

ELISA. Cell culture supernatants were assayed for mouse IL-1 β and TNF (R&D) according to manufacturer's instructions.

Immunoelectron microscopy. For the pre-embedding immuno-EM of cells, PMA-differentiated Flag-Nlrp3-THP1 cells were fixed with 4% PFA for 15 min and were cryoprotected in 2% glycerol and 20% DMSO in PBS. After two freeze-thaw cycles, the cells were blocked in PBS with 0.2% BSA and 0.02% Triton X-100 for 1 h. After washing, the cells were incubated with anti-Flag antibody and gold-conjugated secondary antibody. Silver enhancement was performed by incubating cells with silver enhancement reagent for 1 h in room temperature. After osmification in 0.5% osmium tetroxide for 15 min and dehydration in graded alcohol, the samples were embedded in Durcupan.

Statistical analyses. All values were expressed as the mean \pm s.e.m. of individual samples. Samples were analysed using Student's *t*-test for two groups and ANOVA for multiple groups.

27. Didierlaurent, A. *et al.* Tollip regulates proinflammatory responses to interleukin-1 and lipopolysaccharide. *Mol. Cell. Biol.* **26**, 735–742 (2006).
28. Papin, S. *et al.* The SPRY domain of Pyrin, mutated in familial Mediterranean fever patients, interacts with inflammasome components and inhibits proIL-1 β processing. *Cell Death Differ.* **14**, 1457–1466 (2007).

CORRIGENDUM

doi:10.1038/nature10156

A role for mitochondria in NLRP3 inflammasome activation

Rongbin Zhou, Amir S. Yazdi, Philippe Menu & Jürg Tschopp

Nature **469**, 221–225 (2011)

On page 2 of the print and PDF version of this Letter, there are two citations to Fig. 2f. The first citation to Fig. 2e, f, which refers to active IL-1 β in the culture supernatant after knockdown of beclin 1 and ATG5, should instead be to Fig. 2d, e; the second citation to Fig. 2f, which refers to the stimulation of cells with MSU or nigericin, should be to Fig. 2e. These have been corrected in the HTML version of the manuscript.